Quantifying Thermophysical Properties, Characterization, and Thermal Cycle Testing of Nano-enhanced Organic Eutectic Phase Change Materials for Thermal Energy Storage Applications

Jeeja Jacob[a], A K Pandey[b*], Nasrudin Abd Rahim[a,c*], Jeyraj Selvaraj[a], John Paul[d], M. Samykano[e], R. Saidur[b,f]

[a]Higher Institution Centre of Excellence (HICoE), UM Power Energy Dedicated Advanced Centre (UMPEDAC), Level 4, Wisma R&D, University of Malaya, Jalan Pantai Baharu, 59990 Kuala Lumpur, Malaysia

[b]Research Centre for Nanomaterials and Energy Technology (RCNMET), School of Engineering & Technology, Sunway University, No. 5, Jalan Universiti, Bandar Sunway, Petaling Jaya, 47500 Selangor Darul Ehsan, Malaysia

[c]Renewable Energy Research Group, King Abdulaziz University, Jeddah 21589, Saudi Arabia

[d]Faculty of Mechanical & Automotive Engineering Technology, Universiti Malaysia Pahang, 26600 Pekan, Pahang, Malaysia

[e]College of Engineering, University Malaysia Pahang, Lebuhraya Tun Razak, 26300 Gambang, Kuantan, Pahang, Malaysia

[f]Department of Engineering, Lancaster University, LA1 4YW, United Kingdom

Abstract

Dispersion of highly conductive nanoparticles in Phase Change Materials (PCMs) tends to improve the thermophysical properties of nanocomposites. The current research works condenses the synthesis, chemical, physical, and thermal characterization of novel nano-enhanced eutectic phase change materials (NeUPCMs) dispersed with TiO_2 nanoparticles for thermal management applications. The base matrix primarily comprises of a eutectic of paraffin wax and palmitic acid. Detailed analysis of the uncertainty of each thermophysical property measured was performed. The synthesized nanocomposite logged a maximal thermal conductivity of 0.59 W/mK (2.3-fold as compared with the base-0.25 W/mK) with 0.5% nanofillers. The composites displayed excellent solar transmissivity (82%) as they were doped with nanofillers having a high refractive index. The latent heat of the composites got enhanced by 17% whereas the melting point showed a slight decrement in nanocomposites. Further, zero phase segregation, no subcooling, stable phase transition temperature, and good chemical, and thermal stability were noted from digital scanning calorimetry results with NeUPCMs. The

* Corresponding author: Email (s): adarsh.889@gmail.com; adarshp@sunway.edu.my (A. K. Pandey); nasrudin@um.edu.my (Nasrudin Abd Rahim)

composites exhibited good thermal reliability beyond 500 thermal cycles. It could be potentially deployed in thermal management of medium temperature systems like PV, and PVT systems.

Keywords: Nano-enhanced eutectic phase change material; Thermal conductivity; Latent heat; Thermal energy storage; uncertainty analysis

Highlights

- Novel nanocomposites were synthesized using paraffin wax, palmitic acid, and TiO_2.
- Nanocomposite had a maximal enhancement of 131.5% in thermal conductivity
- 38% rise in solar transmittance when compared with the eutectic base
- Thermophysical properties remained stable even after 500 thermal cycles

Graphical Abstract

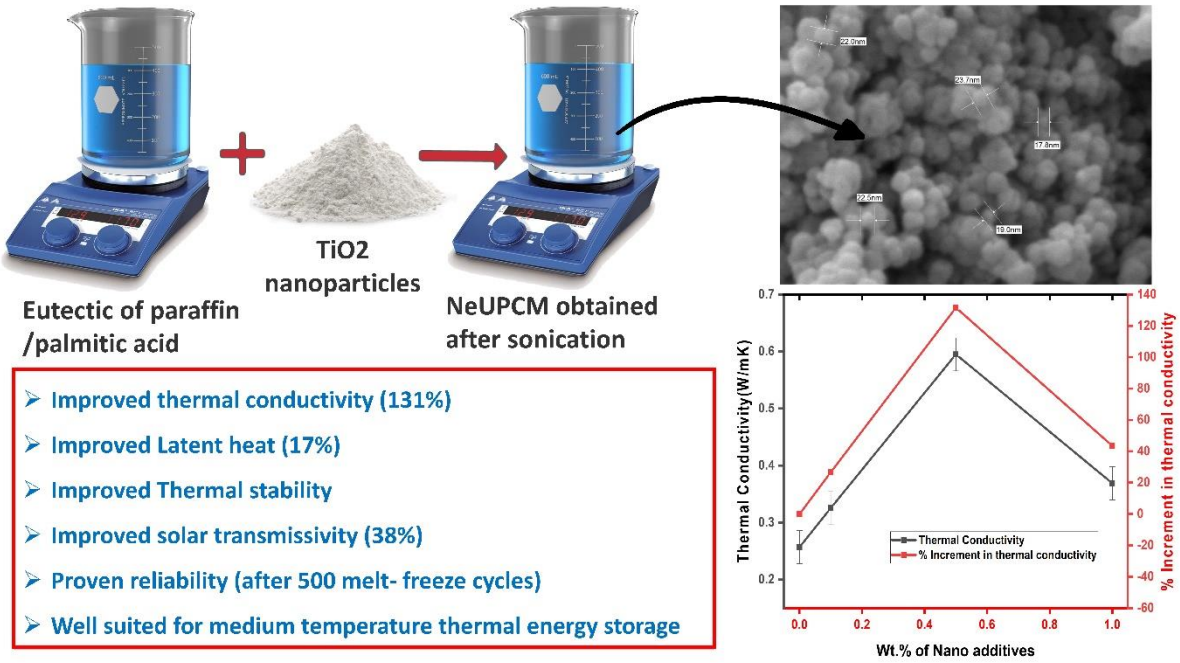

1. Introduction

Energy got elevated to a topic of concern in science prominently owing to sustainability and green concerns. An efficient energy storage technology is needed to combat the intermittencies and instabilities existing in present sustainable and renewable energy sources. Thermal energy storage is gaining importance though heat is the most common form of energy loss [1]. The projected energy demand of the world for the next 20 years is around 27 TW, whereas the earth absorbs 122,000 terawatts of solar irradiation [2]. The seventh sustainable development goal (one among the seventeen laid by the Paris agreement in 2015) stresses the

need to provide cost-effective and green energy for all which is mainly possible by embracing energy-efficient and clean energy sources. Furthermore, as per the energy road map for 2050, the EU proposes renewable energy sources must deliver two-thirds of energy [3]. Thermal energy storage (TES) remains a sustainable solution for solving the issue of energy space-time mismatch. Medium and high-temperature TES system has been extensively deployed in numerical applications like industrial waste heat recovery and solar thermal power plants for thermal management in recent years[4][5]. TES mainly comprises sensible heat storage and latent heat storage [6,7]. Due to its stable output temperature and high heat storage density latent heat energy storage (LHES) outweighs sensible heat energy storage (SHES) [8]. Phase change materials (PCMs) are the basis of LHES as they can absorb and release an immense quantum of heat energy which could be stored during phase transition [9][10]. It must possess a convenient phase transition temperature, excellent heat storage density, good thermal conductivity, lower volume transition ratio, zero corrosion, zero toxicity, zero phase separation/super-cooling degree, phenomenal match with structural materials, and finally economical too [11,12].

Among organic PCMs, paraffin is widely preferred as it possesses a melting temperature within a range. The phase transition temperature and enthalpy of fusion can be altered accordingly by choosing a PCM with more carbon atoms ($CnH2_{n+2}$)[13]. Besides, paraffin is stable both physically and chemically, produced in bulk quantities, cheap, and found in numerous applications related to the solar industry, buildings, and industrial waste management [14]. High-phase transition enthalpy, and the absence of super-cooling, are significant favourable factors favouring fatty acids ($CH_3CH_{2n}COOH$), but they lack thermal conductivity. The phase transition temperature of single fatty acids finds it challenging to meet medium (around 50^0C) temperature solar thermal energy applications. The eutectic PCMs deliver better thermal reliability, latent heat, and comparatively lower phase transition temperatures when compared with individual PCMs. Furthermore, eutectic PCMs can be tuned for any particular melting point as well as latent heat which makes them well suited for any particular application[15]. Dispersing heat pipes, metallic fins, nanoparticles, encapsulation, shape-stabilization, and embedding metal foams are a few techniques adopted for enhancing thermophysical properties. Grafting of functional groups and surface modification of nanomaterials are also adopted, along with the dispersion of zero-dimensional (0D) one-dimensional (1D), two-dimensional (2D), and three-dimensional (3D) structural additives. The term nano additive collectively holds for nanosheets, nanofibers, and nanowires [2]. In most

cases, higher thermal conductivity guarantees rapid energy release in thermal energy storage systems [16]. TiO_2 nanoparticles dispersed in PCMs can improvise the PCM's thermal conductivity [17].

An experimental study was done on the TES characteristics of distinct metal oxide nanoparticles (TiO_2, Al_2O_3, SiO_2, ZnO) dispersed in paraffin wax. Nanocomposite dispersed with TiO_2 logged a significant effect on TC and TES characteristics of paraffin [18]. An analysis of TiO_2/paraffin composites synthesized without surfactant was done. A linear improvement in TC was noted with particle loading, and the trend declined with temperature rise. Post thermal cycling thermophysical characterization properties were lacking [19]. A non-monotonic nature in thermal conductivity enhancement for liquid and solid phases were noted with n-octadecane/TiO_2 composites. The maximal TC enhancement was with 3%wt (solid) of nanofillers. Moreover, when the filler loading exceeded 4% wt. (liquid phase), the TC registered a declining trend. The area of latent heat storage remained untouched [20]. A post thermal cycle analysis on thermal characteristics and stability of paraffin /TiO_2 nanocomposite (in the presence and absence of surfactant) was done. The presence of SSL having a weight ratio of 1:4 (SSL: TiO_2) affected a delay in instability and enhanced the thermal properties of the composite [21]. A prospective shape-stabilized TES material (micro-encapsulated palmitic acid with TiO_2 shell) was prepared through a sol-gel process. The phase transition temperature was maintained, but the latent heat got degraded, and the composite showed good thermal stability [22]. When Palmitic acid/TiO_2 nanocomposites were put to thermophysical characterization, the TC got enhanced by 80%. The composite recorded excellent chemical stability and thermal reliability even after 1500 cycles [23]. When 1.5 wt.% nSiO_2 was dispersed in a eutectic mixture of CA–MA (73.5-26.5 wt.%), thermal conductivity got improved to 142%. The composite's thermal stability got improved, but latent heat had a slight degradation. Even after 2000 cycles, the thermophysical and chemical properties of NePCMs remained stable [24]. The dispersion of n-SiO_2 to a eutectic of CA-PA-SA (79.3:14.7:6.0) lowered the thermal conductivity (034W/mK-0.08W/mK) of FSNePCMs. With nanoparticle dispersion, the melting point and latent heat had a slight decline. The thermophysical and chemical properties of NeUPCMs remained untouched even after 500 cycles [25]. The dispersion of HBN nanofillers onto a eutectic of SA–ODE (2:98 wt.%) yielded a 10% increment in thermal conductivity. The SA–ODE/HBN composites were synthesized and evaluated for their thermophysical properties. The melting point, latent heat, and degree of super-cooling remained almost stationary even with nanoparticle dispersion [26].

A lack of study detailing the synthesis of organic eutectic NePCMs for medium temperature application and its thermophysical characterization was noted down from the literature. The table.1 summarizes the research works conducted on nanocomposites dispersed with TiO_2 nanoparticles. A maximum of 80% increment in thermal conductivity is reported till now. One except other works had reported a decrement in latent heat with TiO_2 dispersion. The present work remains highly relevant as it reports a 131% increment in conductivity without compromising latent heat (17% increment). The composites also exhibited high solar transmissivity primarily due to the inherent refractive index. The results on the stability of nano additives dispersed in eutectic PCM also remain void. The current manuscript demonstrates the synthesis of nano-enhanced organic eutectic (paraffin &palmitic acid) composites dispersed with TiO_2 nanoparticles.

Table.1 Thermal conductivity and enthalpy of TiO_2 dispersed PCMs

Composites dispersed with TiO_2	Thermal conductivity (W/m.K)	Enthalpy (J/g)	Number of thermal cycling's done	Reference
Palmitic acid/TiO_2	80% increment	15.5% decrement	1500	[23]
Paraffin wax/TiO_2	25% increment	15.7% increment	NA	[28]
Octadecane/TiO_2	26% increment	NA	NA	[20]
Stearic acid/TiO_2	70% increment	3.5% decrement	NA	[29]
Paraffin/ TiO_2	13% increment	9% decrement	NA	[19]
(SA + LA)/TiO_2	42% increment	9% decrement	NA	[30]
(PW+PA)/TiO_2	131% increment	17% increment	500	Current work

Even though numerous research works (summarized in table 1) got published that focus mainly on the synthesis and thermophysical characterization of TiO_2 nano-enhanced phase change materials, not a single attempt was made to synthesize a eutectic nanocomposite by dispersing TiO_2 nanoparticles onto paraffin /palmitic eutectic base. In the current work, to the best of the author's knowledge synthesis of eutectic (paraffin wax & palmitic acid) nano enhanced PCM dispersed with TiO_2 nanoparticles remains a novel work. The eutectic PCM displayed comparatively higher thermal conductivity (131%) and a 17% increment in latent heat at 0.5wt% loading rate of nanoparticles than the individual eutectic PCMs. Though the composite showed a slight decrement in phase transition temperature, the enhancement in thermal conductivity without compromising latent heat makes it a potential candidate for TES applications. Furthermore, a detailed morphological analysis, chemical compatibility, thermal

stability, and even thermal reliability for 500 melt-freeze cycles were also performed. Finally, a detailed uncertainty analysis of each thermophysical property measured was also done. The composites displayed excellent solar transmissivity (82%) which makes them suitable for applications like greenhouse heating and desalination. Furthermore, the synthesized TiO_2-based nanocomposites (paraffin/palmitic acid) suit medium-temperature thermal energy storage applications due to their enhanced thermophysical properties (high thermal conductivity and latent heat). This mainly includes PV thermal management, PVT thermal management, desalination (solar still), solar water heating, solar air heating, and thermal management of electronic devices and were reviewed in detail [27][16][2].

2. Experimental section

2.1. Materials

Paraffin wax was procured from RM chemicals (MP-58-60^{0}C). Palmitic acid (PA, with a melting point of 60-62^{0}C, molecular weight-256.43g/mole, analytically pure) was obtained from Sigma Aldrich. SBDS from Sigma Aldrich, TiO_2 (anatase < 25nm, density 3.9g/ml) from Sigma Aldrich.

2.2 Methodology

2.2.1 Synthesis of Palmitic acid /Paraffin Wax binary eutectic Mixture

The PW-PA binary eutectic mixture with a ratio of (60.3/39.7) was prepared by melt-blending method. By using Schroder's equation, the eutectic point of the mixtures was estimated. The required quantity of paraffin wax was measured and melted with the help of a hot plate. Calculated quantities of palmitic acid were added to the melted paraffin while the hot plate temperature was kept above the melting point. The eutectic mixture was mixed homogeneously with the aid of a magnetic stirrer rotating at 500 rpm for 20 minutes. Then the eutectic mixture was allowed to cool down to ambient conditions.

2.2.2 Preparation of nanocomposite eutectic PCM

A two-step method was used for preparing NeUPCMs. The eutectic mixture was heated to 70^{0}C. Then loaded with surfactant (SDBS) and nanoparticles (TiO_2) in the ratio1:1. The liquid mixture was put to probe sonication for 40 minutes, with the sonicator power fixed at 60%. The nano-enhanced eutectic composite with different loading rates of nanoparticles (0%,0.1%,0.5%, and1%) were termed M0-M3. Post sonication, the samples were brought d to

ambient temperature. Figure 1 shows the synthesis route of NeUPCMs and figure 2 shows all the composites (M0-M3).

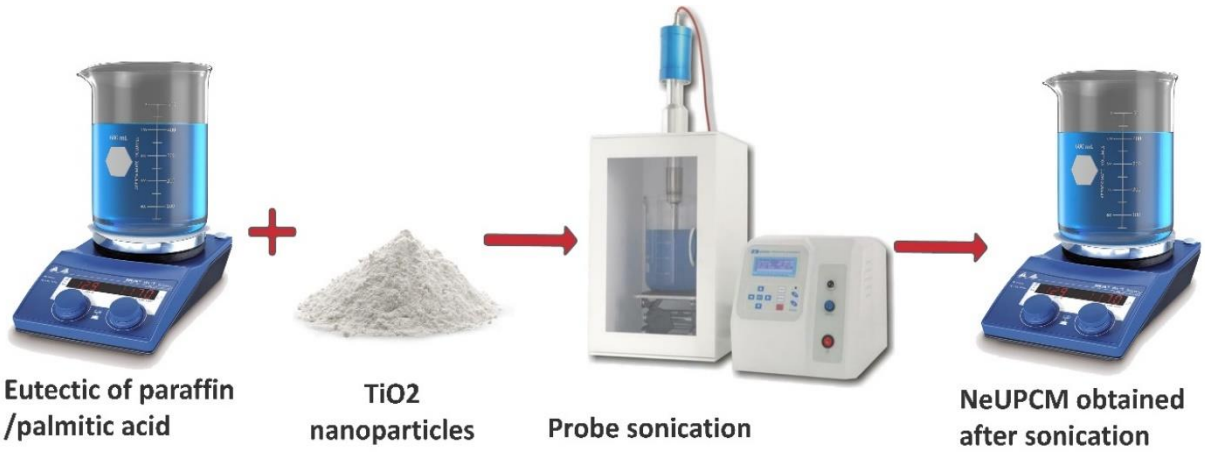

Fig. 1 Synthesis route of nano-enhanced eutectic composites.

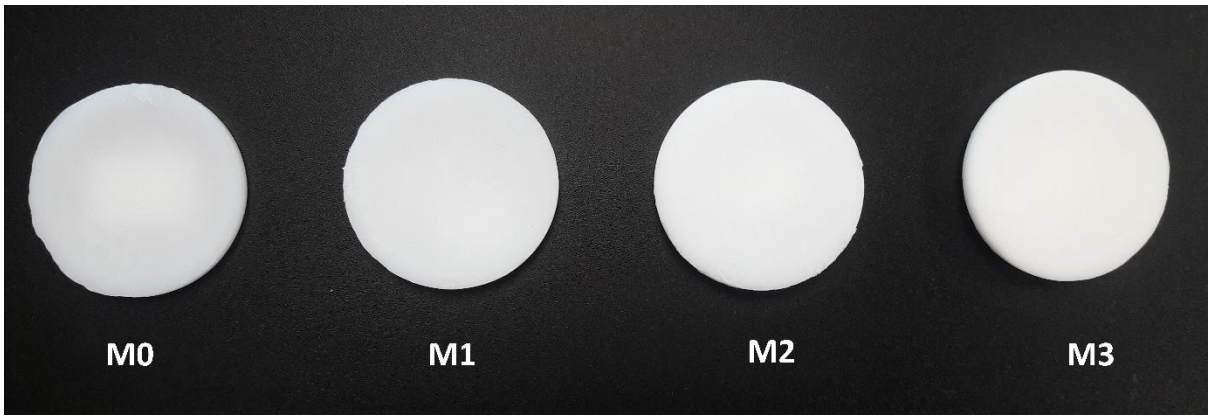

Fig. 2 Synthesised nano-enhanced eutectic composites.

2.2.3. Characterization and instruments

The morphology of TiO_2 nanoparticles and the nanocomposites were inspected with a Field Emission Scanning Electron Microscopy (JSM-IT800, JEOL JAPAN). Fourier Transform Infrared Spectroscopy was utilized in analyzing variations in the functional group of synthesized composites (Spectrum Two FT-IR Spectrometer L160000A, PerkinElmer). The samples were scanned between wavenumber 450 - 4000 cm^{-1} using spectral-grade KBr pellets. With a Perkin Elmer TGA 4000, the thermal stability analysis of the composites were done. The composites were held in a ceramic crucible under an N_2 environment and a heating rate of 10^0C /min. The change in weight of the samples under the TGA furnace was monitored from 30^0C- 450^0C. A UV-VIS spectrometer (LAMBDA 750, PERKIN ELMER) with a range of 200 nm -2000 nm was used to investigate the light transmission capability of the composites. The

crystalline structure of all the samples were investigated using an XRD diffractometer (BRUKER, UK) with Cu Kα radiation at 45 kV and 40 mA. The 2θ range ranged from 10^0-80^0 with a scanning rate of 10^0/minute at ambient temperature. The enthalpy of heating, freezing, melting, and freezing points of samples were estimated with a Differential Scanning Calorimeter Analyzer (DSC-1000-C LINSEIS GERMANY). The evaluations were done under a N_2 atmosphere (flow at 20ml/min.) with a temperature ranging from 30^0C-90^0C with a heating rate of 10^0C/min for heating. A cooling rate of 10^0C/min and a temperature range of 90^0C-30^0C were used for freezing the samples. Thermal conductivity measurement of eutectic PCM and nanocomposites was done with a thermal property analyzer (TEMPOS, Meter-USA) using the transient line heat source method. With an SH-3 sensor, the thermal conductivity and thermal diffusivity were evaluated. The thermal conductivity measurement was done based on ASTMD53314-14 and IEEE 442/D3 standards. Ten readings were taken for each specimen. A time span of 20 minutes was ensured among two consecutive readings to maintain temperature stabilization. A custom-made thermal cycler was used to evaluate the cycling stability. The samples were run between 30^0C-70^0C. The heating was done by a hot gun (2000W STANLEY, STEL 670, type XD02) and cooling was done with Peltier cooling effect.

2.2.4 Uncertainty Analysis

An uncertainty analysis was conducted to nullify the effect of errors that might have occurred while taking measurements. All parameters defining thermal characteristics were measured multiple times, and average values were noted for accurate results. The uncertainty associated with the measuring devices and measured parameters are summarized in table 2. The computed uncertainty associated with each parameter is tabulated in table 3.

Table.2 The uncertainty associated with measuring devices

Equipment	Parameter measured	Uncertainty
TEMPOS	Thermal conductivity	10%
Digital scanning calorimetry	Latent heat	2%
Digital scanning calorimetry	Melting point	0.2^0C
UV-vis	Absorptivity/ Transmissivity	0.1%
Microbalance	Mass of nanoparticles	0.0001gm
Weighing Balance	Mass of PCM	0.001gm
TGA	Temperature	0.3^0C

Table.3 Uncertainty of measured parameters

Measured quantity		Uncertainty			
Sample name	Units	M0	M1	M2	M3
Thermal conductivity	W/m·K	0.058	0.058	0.058	0.058
Diffusivity	mm^2/s	0.0577	0.0577	0.0577	0.0577
Latent heat of melting	kJ/kg	1.85	2.08	2.10	2.16
Latent heat of freezing	kJ/kg	1.71	2.06	1.95	2.05
Melting Point	^0C	0.15	0.15	0.15	0.15
Mass of PCM	gm	0.0012	0.0012	0.0012	0.0012
Mass of SDBS	gm	0.0001	0.0001	0.0001	0.0001

3. Results and Discussions

3.1. Morphology of nanoparticles and NeUPCMs

Nano structural analysis of TiO_2 nanoparticles, pure eutectic composite, and nanocomposite (0.5 Wt.% TiO_2 into paraffin/ palmitic acid) was performed using a FESEM and are shown in Fig.2. As evident from the figure.3(a), spherical-shaped TiO_2 nanoparticles are visible at a magnification of 200,000.

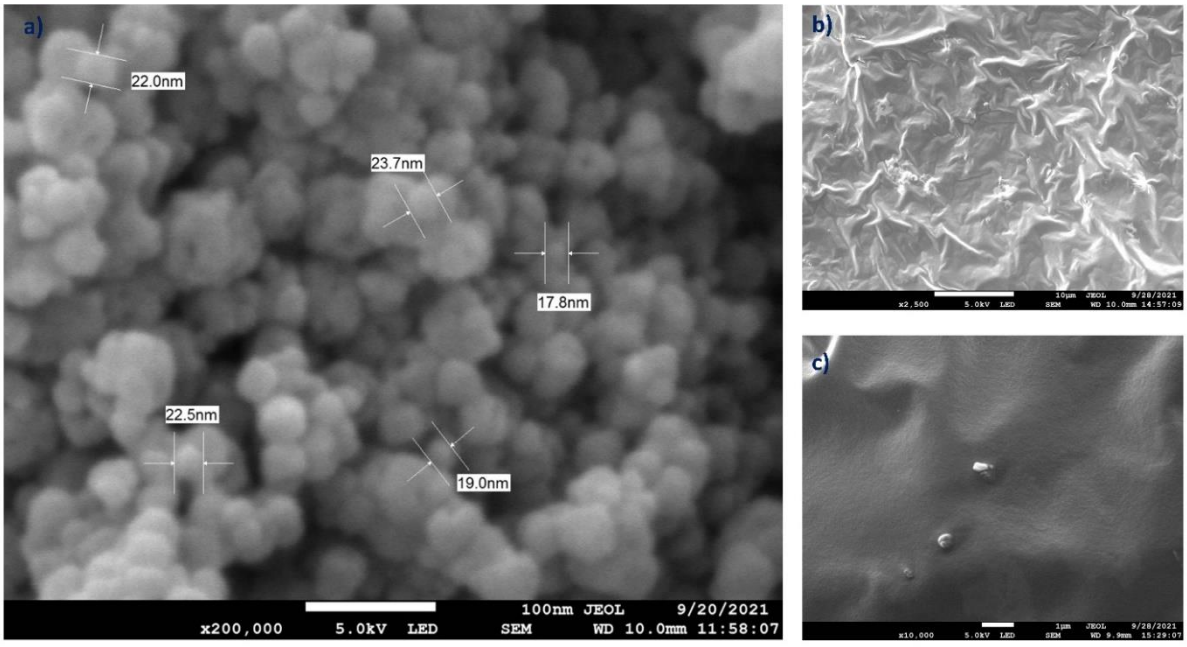

Fig. 3 FE-SEM pictures of (a) TiO_2 nanoparticles, (b) Eutectic PCM, (c) NeUPCMs

These nanoparticles vary from 17-25 nm in size. Much higher magnification of eutectic and nanocomposites was not possible as the composite gets heated up and even melts because of the high intensity of the electron beam. The FESEM image of the eutectic base at 2500 magnification is shown in figure 3 (b) which shows a lamellar layered structure. The homogenous dispersion of TiO_2 nanoparticles in the eutectic base (owing to a repulsive bond of surfactant) is shown in the FE-SEM images (Fig. 3c) and some pores and particles embedded in the eutectic base are also seen.

3.2. Chemical structural Characterisation (FT-IR)

The chemical compatibility of the synthesized nano-enhanced eutectic composites was evaluated with the aid of an FT-IR. The FT-IR curves of nanocomposites, nanoparticles, and surfactant between wavenumbers 4000 to 400 cm^{-1} were plotted in figure 4.

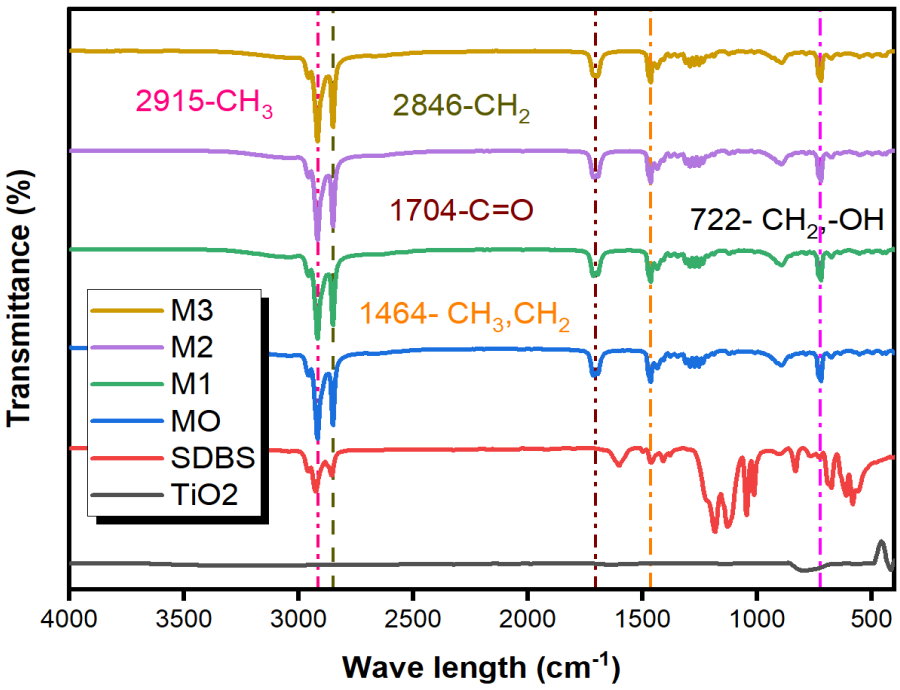

Fig.4 FT-IR Spectrum of the eutectic base, TiO_2, NeUPCMs.

The absorption peaks contributed by palmitic acid in the FT-IR spectrum were detailed in our previous work [10]. Major vibrational shifts were spotted at 2915 & 2846 and were characterized by asymmetrical stretching of CH_3 and CH_2 [31] groups. The pristine eutectic mixture displayed medium vibration bands at 1704, 1464, and 722cm^{-1}. The peak at 1704 cm^{-1} corresponds to a stretching of the C=O bond [23]. The deformation vibration of $–CH_3$ and $–CH_2$ can be marked by a peak at 1464 cm^{-1}. The swinging vibration -OH-[23] & -CH_2-group

were represented by a peak at 722cm^{-1}. The samples M0, M1, M2, and M3 displayed identical FT-IR spectrum above irrespective of TiO_2 nanoparticle loading. Absorption peaks were visible for all samples, and this indicates that the chemical composition of the eutectic mixture remained untouched even with the dispersion of nanoparticles. The nanoparticles were found to be chemically inert and possess good chemical stability. Chemical rearrangements of the functional group were absent in the Spectra, which implies that nanoparticles were chemically inert in the eutectic composite.

3.3. Thermal stability

The thermal stability of nanocomposites stands as a vital parameter for TES applications as the phase transition of nanocomposites normally occur at elevated temperature. TGA curves of nanocomposites (M0-M3) with different additive loading rates are shown in Fig. 5. The degradation particulars (starting degradation temperature -T_5, 5 wt% weight loss, maximal degradation temperature -T_{max}, and the peak temperature of the samples are summarized in table 4. All samples showed a single-stage decomposition and the T_5 and T_{max} are 190.42^{0}C, and 244.53^{0}C, respectively for the pure eutectic. For M2 (sample with maximum thermal conductivity), the T_5 and T_{max} are 207.23^{0}C, and 256.86^{0}C, respectively. Although the initial decomposition temperature of the composites (M1, M2, and M3) showed a wavy nature, it remained higher than the pure eutectic which is acceptable. The maximum decomposition temperature also showed an increasing trend which shows that the samples were synthesized homogenously. It should be noted that the mass loss percentage estimated by TGA remains substantially stable and it, suggests that the TiO_2 nanoparticles got homogeneously dispersed in the eutectic base. A corresponding rise in T_5 and T_{max} value shows an enhancement in the thermal stability of the nanocomposites when dispersed with TiO_2 nanoparticles. The non-uniform dispersion of nanofillers could account for the slight variation. Further, the reason for enhancement is that the intrinsic eutectic matrix possesses extremely excellent thermal stability. Furthermore, nanofillers possess relatively higher specific heat capacity and thermal conductivity values as compared with the eutectic PCM matrix. The weight loss of nanocomposites in a temperature range of 30^{0}C–100^{0}C is mostly similar to pure eutectic composite and it indicates that the synthesized nanocomposites have excellent thermal stability under 100^{0}C, which is quite significant in practical thermal storage applications. Furthermore, the percentage mass loss of the nanocomposite at 400^{0}C is which is lower than pristine eutectic. This was mainly because of the presence of TiO_2 nanoparticles and the capillary, and surface tension forces among the eutectic base and TiO_2 nanoparticles [32]. The non-corrosive nature

of nanocomposites was noticed as the testing pans showed zero destruction. Hence, the prepared nanocomposites have excellent thermal stability and could be deployed in medium-temperature TES applications.

Table.4 Thermal stability parameters for eutectic and nanocomposites

COMPOSITE	$T_{5\%}(^0C)$	T_{max} (^0C)
M0 (PW-PA)	190.4	244.5
M1(PW-PA-0.1%TiO_2)	221.9	280.8
M2(PW-PA-0.5%TiO_2)	207.2	256.9
M3(PW-PA-1.0%TiO_2)	213.2	323.6

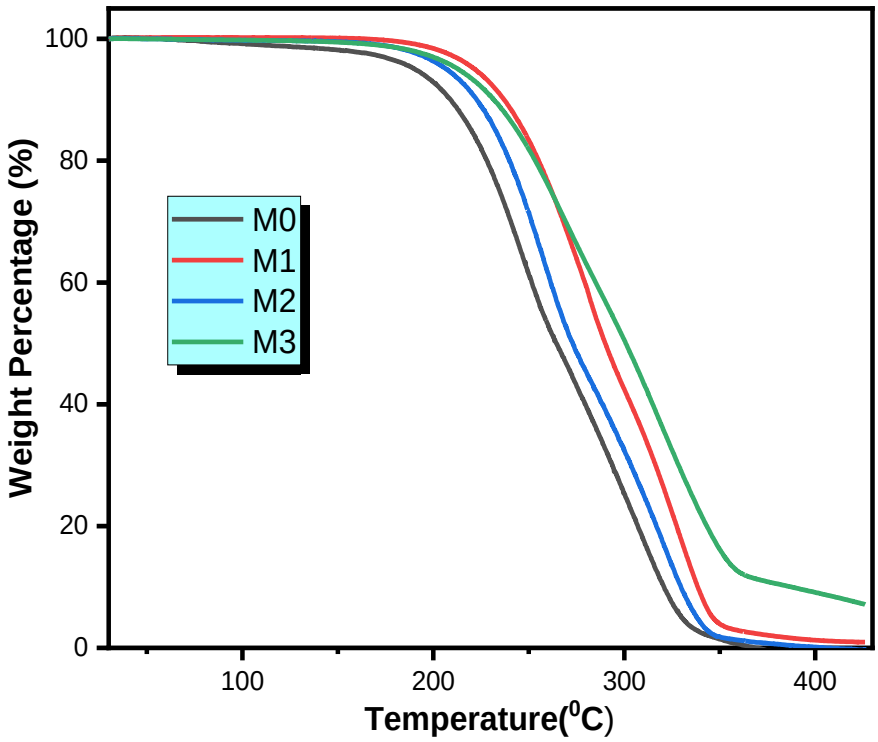

Fig.5 TGA Curves for the composites

3.4. UV–Vis spectral measurement

The light transmission capability of all composites (M0-M3) from the UV–VIS transmission spectrum were compared with extraterrestrial solar spectrum data for analysis. [33]. The UV–VIS spectrum of the composites were plotted in Fig. 6. When compared with the solar spectrum, the transmittance of samples M0, M1, M2, and M3 were 59.53%, 76.27%,

82.45%, and 68.93% respectively. Detailed spectrum-wise solar transmittance values of TiO_2/eutectic nanocomposite are tabulated in Table 5. The transmittance of the composites showed an increment of 28.12% (M1), 38.50% (M2), and 15.79% (M3) with respect to the eutectic base M0 primarily due to the dispersion of TiO_2. The high transmittance of the nanocomposites(even higher than the eutectic) is mainly due to the high refractive index (2.57 for anatase TiO_2) of the nanofillers [34]. The improved transmission capability of the nanocomposites makes it a favourable option for a direct solar thermal applications like greenhouse heating, and desalination.

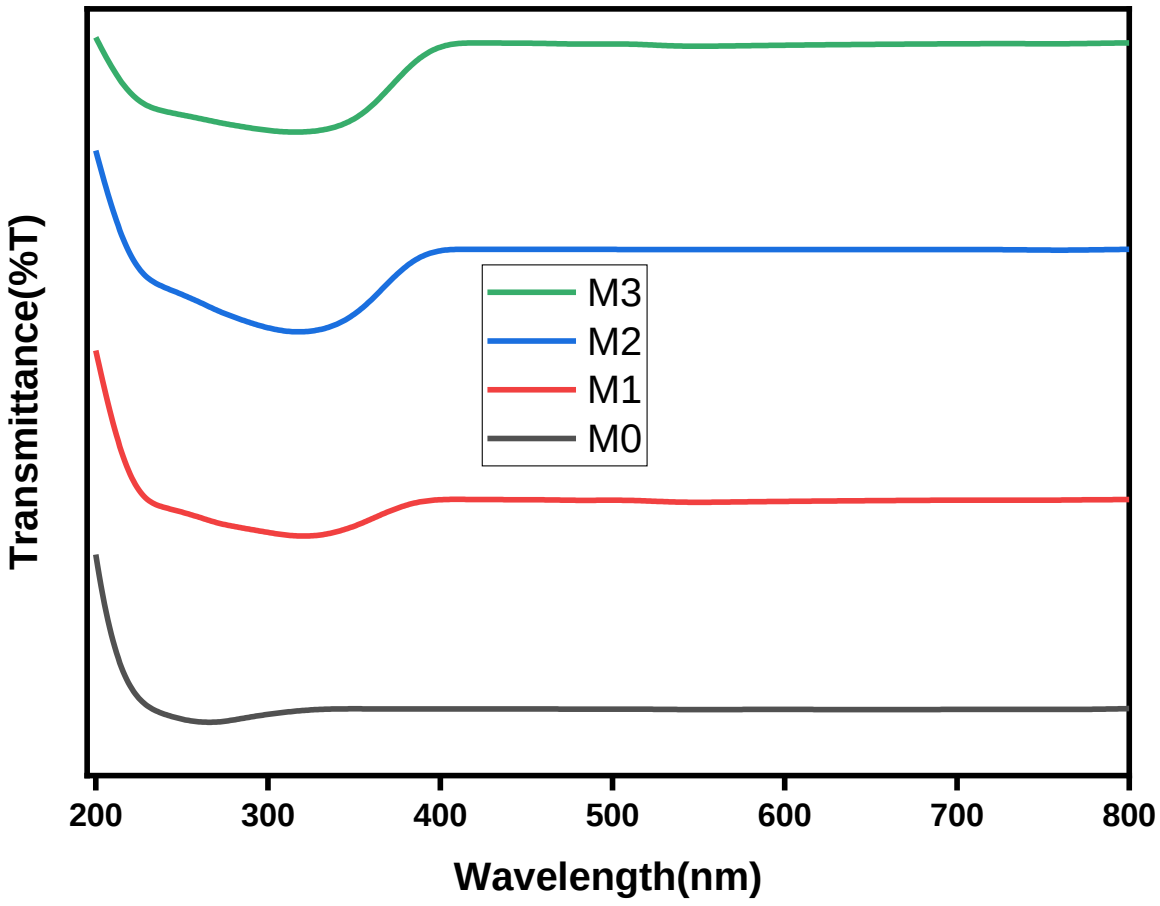

Fig.6 Light transmission curve of composites from wavelength 200 nm -800 nm.

Table.5 Solar transmittance of composites in different spectrum region

SAMPLE	TOTAL	UV	VISIBLE	IR	References
SOLAR spectrum	100%	7%	50%	43%	[35]
M0-0.0%	59.53%	6.28%	80.63%	13.09%	Current work
M1-0.1%	76.27%	6.42%	81.83%	11.75%	Current work

M2-0.5%	82.45%	6.53%	83.84%	9.69%	Current work
M3-1.0%	68.93%	6.69%	85.10%	8.21%	Current work

3.5. XRD analysis

The XRD spectrums of eutectic PCM and nanocomposites are shown in Fig. 7, and it reveals that the pattern is monoclinic. The peaks in the XRD spectrum at 11°, 12°, 21.5°, and 24° were due to the crystalline nature of palmitic acid. These peaks were found to be repetitive in all other samples with TiO_2 nanoparticles. The peak intensity of samples was found slightly varying with different samples, but the peak position remained unchanged. The XRD spectrum results indicate that during the synthesis of NeUPCMs, the crystalline nature of the eutectic base remained the same and the NeUPCMs carry the peaks of PA and TiO_2.

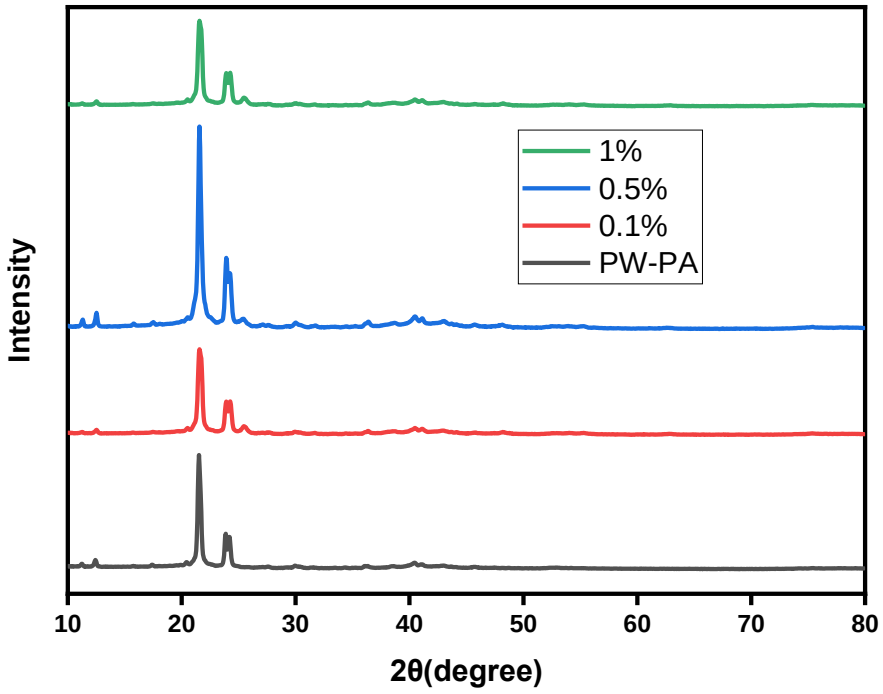

Fig.7 XRD pattern of the composites

3.6. Phase transition temperature and enthalpy

Phase transition temperature and latent heat of the nanocomposites were characterized using DSC. A slight increment in enthalpy for nanocomposites was noted, and it went up with an increment in the loading rate of TiO_2. The thermal storage capacity of the samples was analysed by the term enthalpy efficiency denoted by the term λ. The following expression estimates it

$$\lambda = \frac{\Delta H_{m-NeUPCM}}{\Delta \mathrm{H}_{m-PCM}} \times 100\%$$

The melting enthalpies of PCM and NeUPCMs are denoted by $\Delta \mathrm{H}_{m-PCM}$, $\Delta H_{m-NeUPCM}$ respectively. The λ value reflects the free movement degree of PCM in the [36] composite. A higher λ value indicates a small latent heat loss.

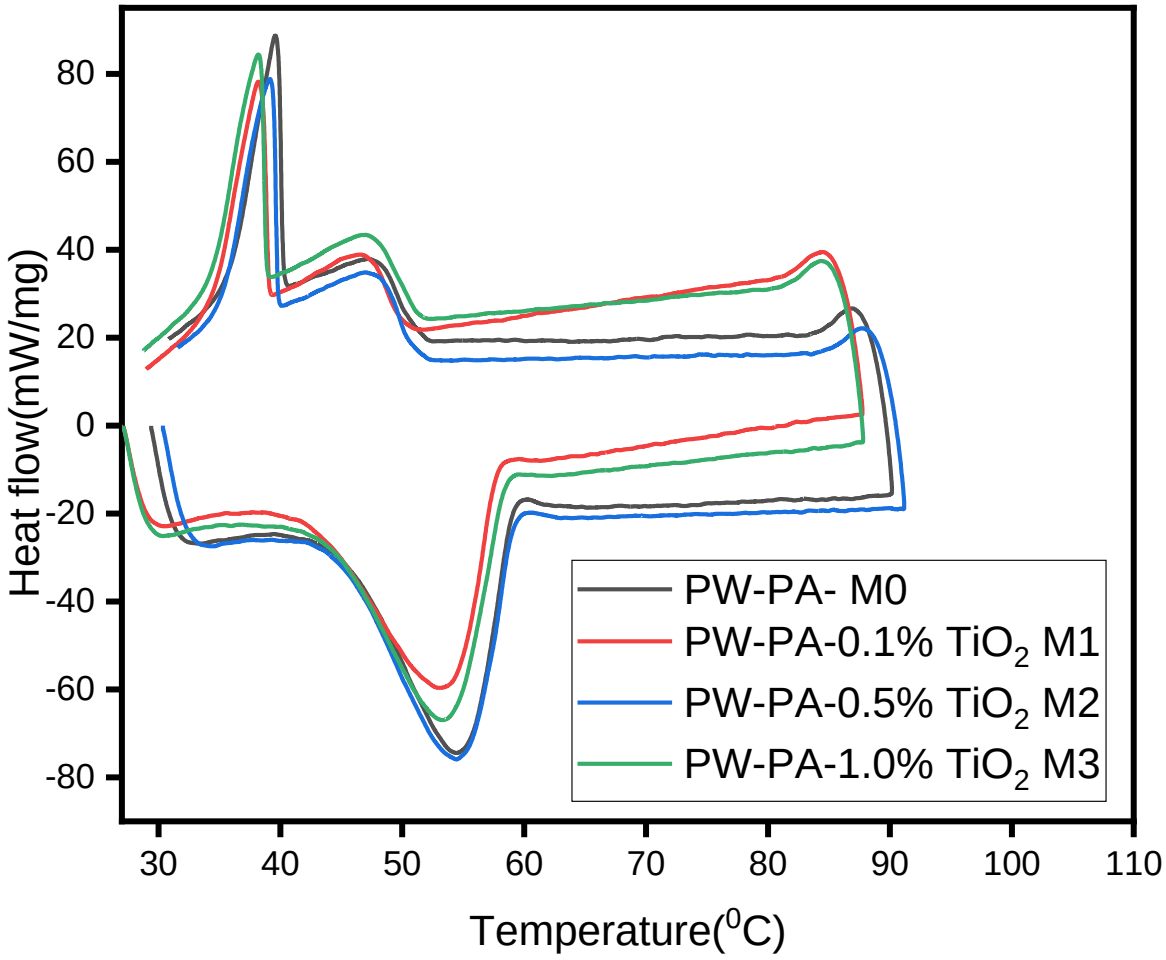

Fig.8 DSC thermogram of composites

The nanocomposite's phase-change performance was evaluated using the term heat storage efficiency and was computed using the following mathematical expression.

$$\gamma = \left(1 - \frac{H_{F.com}}{H_{M.com}}\right) * 100\%$$

Melting & freezing enthalpies were denoted by $H_{M.com}$ and $H_{F.com}$ respectively. The higher melting enthalpy in the nanocomposites could be due to the quality loss during the melting in DSC [37]. A lower γ value denotes a higher heat storage efficiency [36].

The crystallization factor is a reflector for the interaction between PCM and the supporting material. It also corrects the influence of PCM percentage on the phase transition latent heat [38]. The crystallinity factor reveals the phase transition behavior of the PCM matrix in the fillers and is estimated by the below-given equation [39].

$$F_C = \frac{\Delta H_{NeUPCM}}{\Delta H_{PURE}\beta} * 100\%$$

ΔH_{NeUPCM} denotes the enthalpy of the eutectic nano PCM, ΔH_{PURE} denotes the enthalpy of pure PCM, β corresponds to the mass fraction of PCM in the composite. Comparatively higher crystallization ratio results in phenomenal liquidation and solidification enthalpies [39]. A comparatively lower Fc value for nanocomposite indicates that more particles were confined (disordered) by the PCM. The restrained PCMs fail to crystallize and will not contribute to TES [40].

The term effective energy stored per unit mass of PCM was employed to assess the effectiveness of the PCM matrix in different nanocomposites. The following mathematical relation gives the expression for efficient energy per unit mass of phase change material

$$E_{ef} = \Delta H_{PCM} * \left[\frac{\Delta H_{NeUPCM}}{\Delta H_{PURE}\beta} * 100\%\right]$$

$$E_{ef} = F_C * \Delta H_{NeUPCM}$$

A comparatively higher value of E_{ef} indicates a rather free movement of liquid PCM in the porous network which remains advantageous to the heating-cooling enthalpy of nanocomposite [39]. The enthalpy and phase transition temperatures of all composites are detailed in Tables 6 and 7. A rise in enthalpy is primarily due to the larger surface area of TiO_2 nanoparticles, which causes an intermolecular interaction between the eutectic base and nanofillers. Van der Waals forces also tend to contribute toward intermolecular interaction between the nanofillers and eutectic PCM [41]. Phonon motion, the surface charge of dispersed nanomaterials, and also the layering in the liquid-solid phase attributes to an enhanced heating enthalpy [28].

Table.6 Melting and freezing point of composites

Sample	Melting point			Freezing Point		
	T_{on} (^{0}C)	T_m (^{0}C)	T_{end} (^{0}C)	T_{on} (^{0}C)	T_f (^{0}C)	T_{end} (^{0}C)
M0-0.0%	38.1*	55.0*	61.4 *	29.8*	37.6*	52.3*

M1-0.1%	38.6*	53.3*	59.3 *	29.9*	38.2*	51.6*
M2-0.5%	37.3 *	53.7*	61.0*	29.3*	38.0*	51.9*
M3-1.0%	38.9 *	53.4*	58.9*	28.8*	38.2*	51.7*

* Error of 0.15

Table.7 Latent heat of composites

Sample	Melting enthalpy ΔH_m (kJ/Kg)	Freezing enthalpy ΔH_F (kJ/Kg)	Heat storage efficiency	Enthalpy efficiency (%)	Crystallisation factor (%)	Efficient energy per unit mass of PCM[39] (kJ/kg)
M0-0.0%	160.0±1.85	148.0±1.71	7.5	-	-	-
M1-0.1%	179.7±2.08	177.8±2.06	1.1	112.4	112.5	179.9
M2-0.5%	181.4±2.10	168.4±1.95	7.2	113.4	114	182.3
M3-1.0%	187.2±2.16	177.1±2.05	5.4	117	118.2	189.1

3.7. Thermal conductivity of nanocomposites

Thermal conductivity remains a significant factor in the TES context. The synthesized nanocomposites exhibit enhanced thermal conductivity when compared with the eutectic PCM. The thermal conductivity of the prepared nanocomposites are tabulated in table 8**.** The thermal conductivity was found to be maximum (increment of 131.5%) for sample M3, which carried a nanoparticle loading rate of 0.5%. A reduction in thermal conductivity was noted down for the 1.0% loading of TiO_2 nanoparticles. Reduction in thermal conductivity along with increment in nanofiller loading was reported in many cases. This decremental trend is primarily due to the agglomeration of nanoparticles, which led to the formation of a heterogeneous composite. The composites with higher loading of nanoparticles fail to establish a continuous thermal network, which generally enhances the conductivity with nanoparticle addition [42]. The TiO_2 nanoparticles possess a lower size, density, and even high surface area. Hence, they possess a more substantial degree of homogenization and dispersion rate into the eutectic PCM matrix. Furthermore, the boundary layer thermal resistance of nanofillers and lattice molecules of eutectic PCM contributes significantly to the changes in thermal conductivity results [58]. Normally, the following significant factors result in an improved thermal conductance within the NeUPCMs. The phenomenal thermal conductivity of nanofillers and the movement of the

nanofillers within NeUPCMs in liquid-phase results in a quasi-convection phenomenon [43]. The enhancement in thermal conductivity ensures shorter heat storage and release timings for the composites. The mechanism of thermal transport in a perfect crystal is explained with the help of phonon transport. Phonon motion is comparatively slower in the PCM matrix mainly because of the absence of interaction between atoms in a PCM and irregular molecular alignment during phase transition [44].

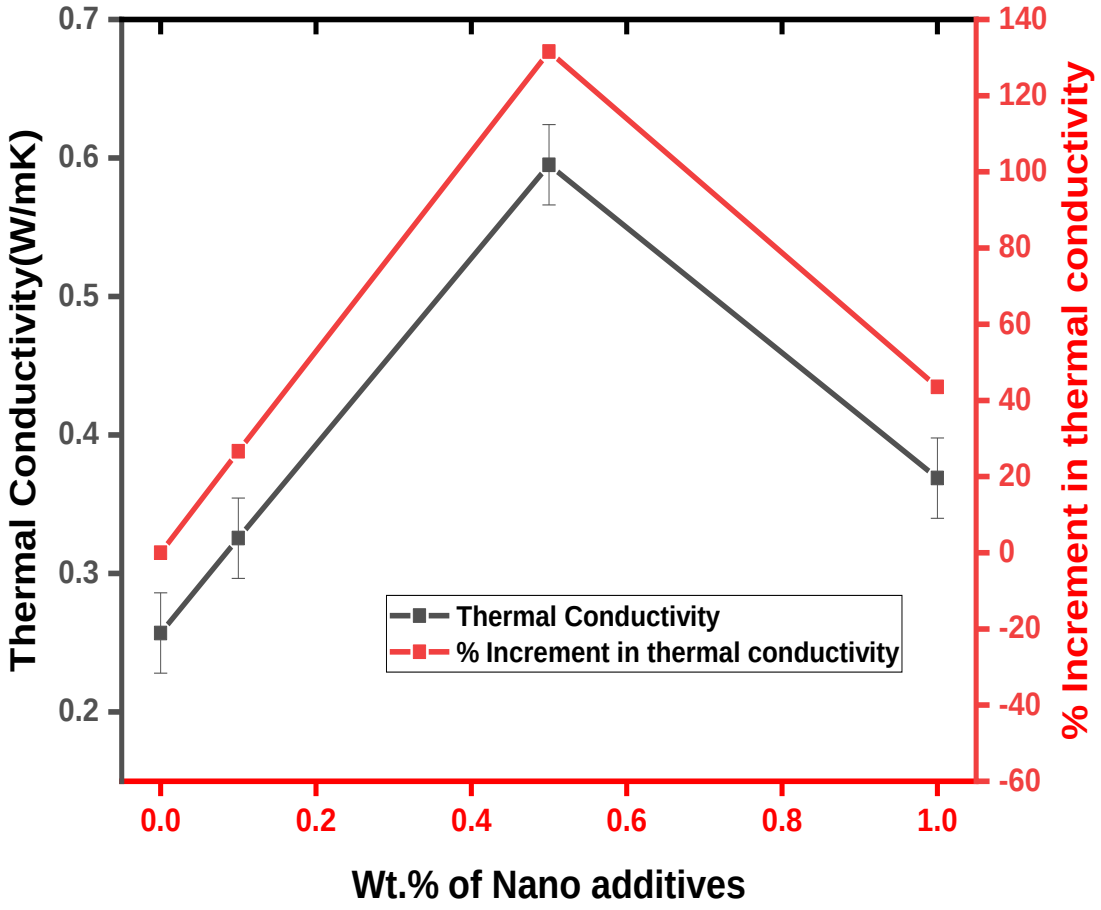

Fig.9. Thermal conductivity of composites at room temperature.

An enhancement in thermal conductivity can be noted by long-distance phonon motion in a particular direction within the eutectic PCM matrix. The nanoparticle dispersion curtails the void space in the eutectic PCM matrix and improves thermal conductivity [45]. A favourable hike in thermal conductivity was reported with TiO_2 nanoparticles mainly due to spherical shape and sensational dispersion; it displays great attraction between nanofillers and the eutectic matrix [20]. A detailed Microstructural analysis of the nano-enhanced eutectic composite must be conducted to analyze the trend in thermal conductivity.

Table.8 Experimental values for diffusivity and thermal conductivity of synthesised composites

Samples	Mean thermal conductivity of samples	Increment in Thermal Conductivity	Mean Diffusivity samples	Decrement in Diffusivity
	(W/m.K)	%	mm^2/s	%
M0	0.257±0.058	---	0.248 ±0.058	---
M1	0.326±.0058	26.65	0.148±0.058	40
M2	0.595±0.058	131.55	0.201±0.058	19
M3	0.369±0.058	43.54	0.167±0.058	33

3.8. Thermal cycling test

The thermal stability of the prepared eutectic base and the best composite (with maximal thermal conductivity) were evaluated by a custom-made thermal cycler. The thermal cycler comprises three chambers that operate in a temperature range of 30^0C-100^0C. An airflow initiated by a Peltier cooling cools the samples. The samples were placed in an aluminium crucible and were run between 30^0C -70^0C. the peak temperature was kept slightly above the melting point to ensure the melting of the entire mass of the sample. The samples were melted using a heating gun directly placed below the crucible. The heater gets cut- off once the maximum set temperature is attained which is followed by a cooling current. The peak set temperature is attained within 3 min whereas the cooling cycle takes a slightly longer duration about 8 min. The shorter heating and cooling duration is mainly due to the less quantity of samples taken (approximately 1000 mg). The samples taken for cycling are M0 (base) and M2 (maximum conductivity). Moderate cycling of 500 no's was performed on the samples to analyze their thermal stability and reliability. Figs. 10 and 11 show the FTIR spectrum and DSC curve for the base and the M2 samples. The FTIR spectrum remains identical even after 500 cycles for the samples (M0 and M2).

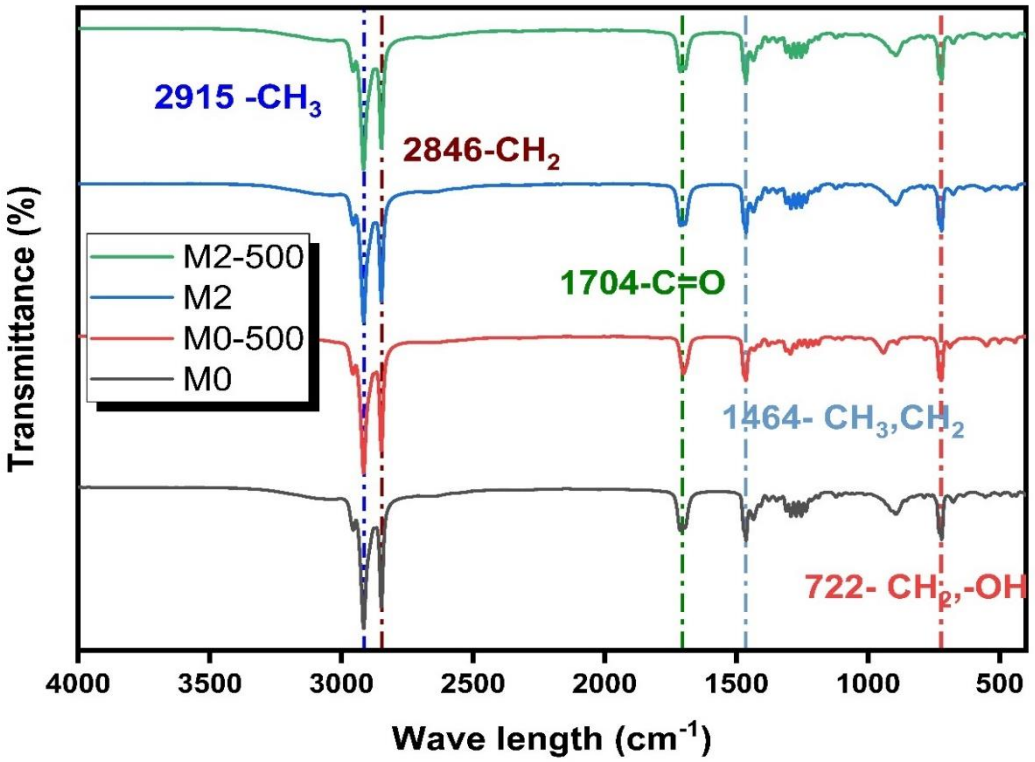

Fig. 10. FT-IR Spectrum of PW-PA, PW-PA-0.5% TiO_2 after 0 and 500 thermal cycles.

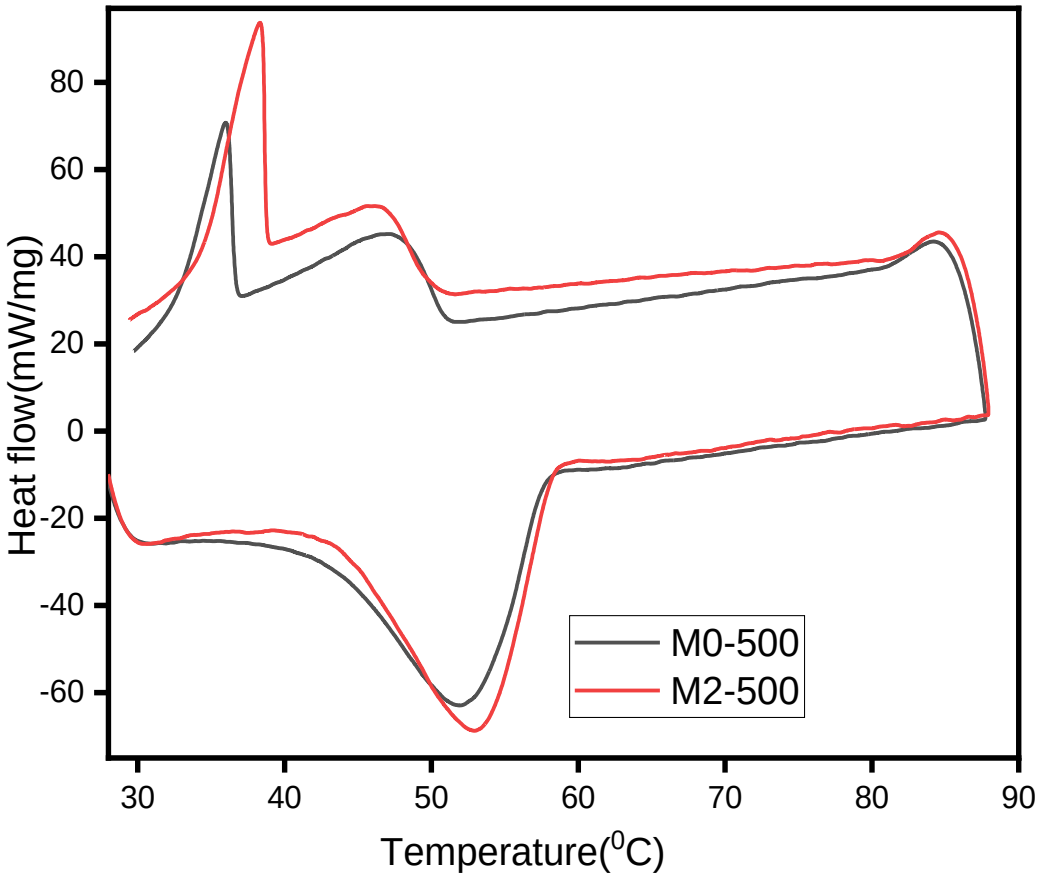

Fig. 11. DSC curve of PW-PA, PW-PA-0.5% TiO_2 after 500 thermal cycles.

The chemical stability could be ensured as new peaks were absent in the FTIR spectrum of cycled samples. A detailed study of TGA thermograms also revealed identical results for cycled and uncycled samples. The initial decomposition temperature of cycled and uncycled eutectic base took place hardly at similar temperatures. The maximum decomposition temperature also showed a similar pattern. The enthalpy and phase transition values of the composites are condensed in Table 9 and the values (latent heat and phase transition temperatures) remained almost constant (before and after cycling). The thermal cycling results evidently show that the chemical and thermal stability of the eutectic nanocomposite can be efficiently utilized for thermal energy storage applications. The novel composite can deliver better performance owing to its improved thermal conductivity when compared with the eutectic base.

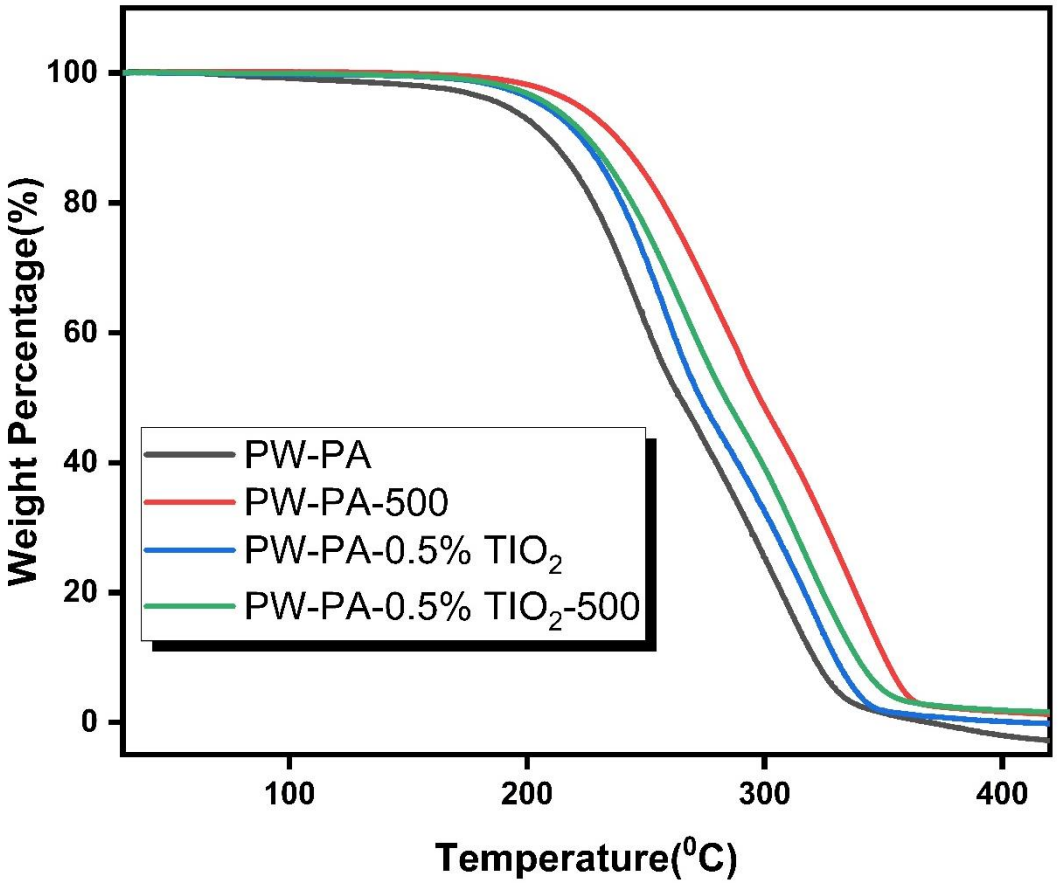

Fig.12. TGA curves of PW-PA, PW-PA-0.5% TiO_2 after 0 and 500 thermal cycles.

Table.9: Latent heat and phase transition temperature of cycled composites

Sample	Melting point T_m (^{0}C)	Freezing Point T_f (^{0}C)	Melting enthalpy ΔH_m (KJ/Kg)	Freezing enthalpy ΔH_F (KJ/Kg)
M0-0.0%$_{500}$	53.01±0.15	35.99±0.15	159.07±1.84	149.02±1.72
M2-0.5%$_{500}$	52.05±0.15	38.31±0.15	180.23±2.08	177.08±2.05

4. Conclusion

In this experimental study, nano-enhanced eutectic composites were synthesized by dispersing TiO_2 nanoparticles in paraffin wax palmitic binary eutectic mixture (Schroder's equation) by two-step method (ultrasonication). The experimental work mainly focused on improving the thermophysical properties, especially the thermal conductivity as it remains crucial in thermal energy storage applications. The reliability and stability of the samples were analyzed after thermal cycling (melt-freeze cycle) of 500 cycles. A comparison of thermo-physical properties of nanocomposites dispersed with TiO_2 nanoparticles is given in Table 1. The thermophysical characterization of the novel eutectic nanocomposite was done and the significant findings are discussed below:

1. The novel eutectic nanocomposite recorded an increment in latent heat when compared with base (17%). An increment in latent heat for a nanocomposite is highly advantageous as it can store more heat with the same quantity of PCM.
2. Thermal conductivity got improved by 2.3 folds with the dispersion of TiO_2 nanoparticles. A rise in thermal conductivity causes a decline in interfacial thermal resistance, which enhances the charging efficiency of PCM when deployed for TES applications.
3. The reliability and stability of the composites were established by accelerated thermal cycling performed for 500 cycles.
4. The maximum solar transmissivity of nanocomposites is around, 82%, The higher refractive index of TiO_2 accounts for a higher transmissivity of the nanocomposites which is highly useful in applications like greenhouse heating

The summarized thermophysical characterization results confirm an improvement in physical,

and thermal properties, particularly thermal conductivity, enthalpy, and even thermal stability. Furthermore, the composite has got excellent thermal energy storage potential. The melting and freezing point of the sample is between 37-55^{0}C. The synthesized sample could be deployed in numerous applications like thermal management of electronic devices, solar still, solar cookers, solar air heaters, solar domestic heaters, etc. Moreover, the range of applications could be further extended toward waste heat recovery units like heat exchangers, regenerator devices, and even batteries. This work may provide a new idea to fabricate nanocomposites, presenting a broader application in the fields of highly thermally conductive and solar spectrum transmission capabilities. In conclusion, with the dispersion of TiO_2 onto eutectic PCM, next-generation binary nanocomposite with excellent heat storage and solar transmissivity was successfully developed. It is expected that a wider range of applications can be attained with the synthesis of the next-generation organic eutectic NeUPCMs.

Acknowledgment

The authors acknowledge the financial assistance of Sunway University through Sunway University collaborative research fund: MRU 2019 (STR-RMF-MRU-004-2019), and Universiti Malaysia Pahang (UMP) for the financial assistance provided under the Doctoral Research Scheme for carrying out this research. The authors also thank the technical and financial assistance of UM Power Energy Dedicated Advanced Centre (UMPEDAC) and the Higher Institution Centre of Excellence (HICoE) Program Research Grant, UMPEDAC-2018 (MOHE HICOE-UMPEDAC), Ministry of Education Malaysia, TOP100UMPEDAC, RU012-2019, University of Malaya. Also, Toyota classic 2018 fund by Toyota UMW Sdn Bhd-Development of innovative technology for solar photovoltaic thermal cooling system PVU001-2019 is duly acknowledged.

Declaration of Competing Interests

The authors declare that they have no known competing financial interests or personal relationships that could have appeared to influence the work reported in this paper.

Data Availability

Data will be made available on request.

Credit Author Statement

Jeeja Jacob: Data Curation, Investigation, Formal analysis, Writing - Original Draft

A K Pandey: Conceptualization, Methodology, Formal analysis, Validation, Funding acquisition, Supervision

Nasrudin Abd Rahim: Funding acquisition, Writing - Review & Editing, Supervision

Jeyraj Selvaraj: Funding acquisition, Writing - Review & Editing, Supervision

John Paul: Formal analysis, Data Curation, Writing - Review & Editing

M. Samykano: Writing - Review & Editing, Methodology

R. Saidur: Review & Editing, Resources, Investigation

References

[1] M. Graham, J. Smith, M. Bilton, E. Shchukina, A.A. Novikov, V. Vinokurov, D.G. Shchukin, Highly Stable Energy Capsules with Nano-SiO2Pickering Shell for Thermal Energy Storage and Release, ACS Nano. 14 (2020) 8894–8901. https://doi.org/10.1021/acsnano.0c03706.

[2] J. Paul, K. Kadirgama, M. Samykano, A.K. Pandey, V. V. Tyagi, A comprehensive review on thermophysical properties and solar thermal applications of organic nano composite phase change materials, J. Energy Storage. 45 (2022) 103415. https://doi.org/10.1016/j.est.2021.103415.

[3] J. Jacob, A.K. Pandey, N.A. Rahim, J. Selvaraj, M. Samykano, R. Saidur, V.V. Tyagi, Concentrated Photovoltaic Thermal (CPVT) systems: Recent advancements in clean energy applications, thermal management and storage, J. Energy Storage. (2021) 103369. https://doi.org/10.1016/j.est.2021.103369.

[4] B. Cárdenas, N. León, High temperature latent heat thermal energy storage: Phase change materials, design considerations and performance enhancement techniques, Renew. Sustain. Energy Rev. 27 (2013) 724–737. https://doi.org/10.1016/j.rser.2013.07.028.

[5] T. Nomura, T. Akiyama, High-temperature latent heat storage technology to utilize exergy of solar heat and industrial exhaust heat, Green Energy Technol. (2018) 1207–1224. https://doi.org/10.1007/978-3-319-62572-0_77.

[6] P. Zhang, X. Xiao, Z.W. Ma, A review of the composite phase change materials: Fabrication, characterization, mathematical modeling and application to performance enhancement, Appl. Energy. 165 (2016) 472–510. https://doi.org/10.1016/j.apenergy.2015.12.043.

[7] W. Zhao, D.M. France, W. Yu, T. Kim, D. Singh, Phase change material with graphite

foam for applications in high-temperature latent heat storage systems of concentrated solar power plants, Renew. Energy. 69 (2014) 134–146. https://doi.org/10.1016/j.renene.2014.03.031.

[8] H. Zhang, L. Zhang, Q. Li, C. Huang, H. Guo, L. Xiong, X. Chen, Preparation and characterization of methyl palmitate/palygorskite composite phase change material for thermal energy storage in buildings, Constr. Build. Mater. 226 (2019) 212–219. https://doi.org/10.1016/j.conbuildmat.2019.07.152.

[9] T. Rehman, H.M. Ali, M.M. Janjua, U. Sajjad, W.M. Yan, A critical review on heat transfer augmentation of phase change materials embedded with porous materials/foams, Int. J. Heat Mass Transf. 135 (2019) 649–673. https://doi.org/10.1016/j.ijheatmasstransfer.2019.02.001.

[10] J. Jacob, A.K. Pandey, N.A. Rahim, J. Selvaraj, M. Samykano, V.V. Tyagi, R. Saidur, Investigation on thermophysical properties of metallic oxide nanoparticle dispersed in fatty acid, Mater. Today Proc. 47 (2021) 2864–2868. https://doi.org/10.1016/j.matpr.2021.03.639.

[11] Z.A. Qureshi, H.M. Ali, S. Khushnood, Recent advances on thermal conductivity enhancement of phase change materials for energy storage system: A review, Int. J. Heat Mass Transf. 127 (2018) 838–856. https://doi.org/10.1016/j.ijheatmasstransfer.2018.08.049.

[12] M.M.A. Khan, N.I. Ibrahim, I.M. Mahbubul, H. Muhammad. Ali, R. Saidur, F.A. Al-Sulaiman, Evaluation of solar collector designs with integrated latent heat thermal energy storage: A review, Sol. Energy. 166 (2018) 334–350. https://doi.org/10.1016/j.solener.2018.03.014.

[13] A. Reyes, L. Henríquez-Vargas, J. Vásquez, N. Pailahueque, G. Aguilar, Analysis of a laboratory scale thermal energy accumulator using two-phases heterogeneous paraffin wax-water mixtures, Renew. Energy. 145 (2020) 41–51. https://doi.org/10.1016/j.renene.2019.06.007.

[14] R. Li, Y. Zhou, X. Duan, A novel composite phase change material with paraffin wax in tailings porous ceramics, Appl. Therm. Eng. 151 (2019) 115–123. https://doi.org/10.1016/j.applthermaleng.2019.01.104.

[15] Z. Hu, C. Wang, W. Jia, X. Li, Z. Cai, Preparation and Thermal Properties of 1-Hexadecanol-Palmitic Acid Eutectic Mixture/Activated Carbon Composite Phase Change Material for Thermal Energy Storage, ChemistrySelect. 4 (2019) 222–227. https://doi.org/10.1002/slct.201801773.

[16] J. Paul, A.K. Pandey, Y.N. Mishra, Z. Said, Y.K. Mishra, Z. Ma, J. Jacob, K. Kadirgama, M. Samykano, V. V. Tyagi, Nano-enhanced organic form stable PCMs for medium temperature solar thermal energy harvesting: Recent progresses, challenges, and opportunities, Renew. Sustain. Energy Rev. 161 (2022) 112321. https://doi.org/10.1016/j.rser.2022.112321.

[17] X. Chen, Z. Tang, P. Liu, H. Gao, Y. Chang, G. Wang, Smart Utilization of Multifunctional Metal Oxides in Phase Change Materials, Matter. 3 (2020) 708–741. https://doi.org/10.1016/j.matt.2020.05.016.

[18] T.P. Teng, C.C. Yu, Characteristics of phase-change materials containing oxide nano-additives for thermal storage, Nanoscale Res. Lett. 7 (2012) 1–10. https://doi.org/10.1186/1556-276X-7-611.

[19] J. Wang, H. Xie, Z. Guo, L. Guan, Y. Li, Improved thermal properties of paraffin wax by the addition of TiO2 nanoparticles, Appl. Therm. Eng. 73 (2014) 1541–1547. https://doi.org/10.1016/j.applthermaleng.2014.05.078.

[20] S. Motahar, N. Nikkam, A.A. Alemrajabi, R. Khodabandeh, M.S. Toprak, M. Muhammed, Experimental investigation on thermal and rheological properties of n-octadecane with dispersed TiO2 nanoparticles, Int. Commun. Heat Mass Transf. 59 (2014) 68–74. https://doi.org/10.1016/j.icheatmasstransfer.2014.10.016.

[21] S. Sami, N. Etesami, Improving thermal characteristics and stability of phase change material containing TiO2 nanoparticles after thermal cycles for energy storage, Appl. Therm. Eng. 124 (2017) 346–352. https://doi.org/10.1016/j.applthermaleng.2017.06.023.

[22] L. Cao, F. Tang, G. Fang, Preparation and characteristics of microencapsulated palmitic acid with TiO2 shell as shape-stabilized thermal energy storage materials, Sol. Energy Mater. Sol. Cells. 123 (2014) 183–188. https://doi.org/10.1016/j.solmat.2014.01.023.

[23] R.K. Sharma, P. Ganesan, V. V. Tyagi, H.S.C. Metselaar, S.C. Sandaran, Thermal properties and heat storage analysis of palmitic acid-TiO2 composite as nano-enhanced organic phase change material (NEOPCM), Appl. Therm. Eng. 99 (2016) 1254–1262. https://doi.org/10.1016/j.applthermaleng.2016.01.130.

[24] M. Martín, A. Villalba, A.I. Fernández, C. Barreneche, Energy & Buildings Development of new nano-enhanced phase change materials (NEPCM) to improve energy efficiency in buildings : Lab-scale characterization, Energy Build. 192 (2019) 75–83. https://doi.org/10.1016/j.enbuild.2019.03.029.

[25] Z. Luo, H. Zhang, X. Gao, T. Xu, Y. Fang, Z. Zhang, Fabrication and characterization of form-stable capric-palmitic-stearic acid ternary eutectic mixture/nano-SiO2 composite phase change material, Energy Build. 147 (2017) 41–46. https://doi.org/10.1016/j.enbuild.2017.04.005.

[26] D. Su, Y. Jia, G. Alva, F. Tang, G. Fang, Preparation and thermal properties of n – octadecane / stearic acid eutectic mixtures with hexagonal boron nitride as phase change materials for thermal energy storage, Energy Build. 131 (2016) 35–41. https://doi.org/10.1016/j.enbuild.2016.09.022.

[27] J. Paul, K. Kadirgama, M. Samykano, R. Saidur, A.K. Pandey, R. V Mohan, An Updated Review on Low-Temperature Nanocomposites with a Special Focus on Thermal Management in Buildings, Energy Eng. 119 (2022) 1300–1325. https://doi.org/10.32604/ee.2022.019172.

[28] D. Dsilva Winfred Rufuss, L. Suganthi, S. Iniyan, P.A. Davies, Effects of nanoparticle-enhanced phase change material (NPCM) on solar still productivity, J. Clean. Prod. 192 (2018) 9–29. https://doi.org/10.1016/j.jclepro.2018.04.201.

[29] S. Harikrishnan, S. Magesh, S. Kalaiselvam, Preparation and thermal energy storage behaviour of stearic acid-TiO 2 nanofluids as a phase change material for solar heating systems, Thermochim. Acta. 565 (2013) 137–145. https://doi.org/10.1016/j.tca.2013.05.001.

[30] S. Harikrishnan, M. Deenadhayalan, S. Kalaiselvam, Experimental investigation of solidification and melting characteristics of composite PCMs for building heating application, Energy Convers. Manag. 86 (2014) 864–872. https://doi.org/10.1016/j.enconman.2014.06.042.

[31] N. Mekaddem, S. Ben Ali, M. Fois, A. Hannachi, Paraffin/expanded perlite/plaster as thermal energy storage composite, Energy Procedia. 157 (2019) 1118–1129. https://doi.org/10.1016/j.egypro.2018.11.279.

[32] Y. Guo, Z. Lyu, X. Yang, Y. Lu, K. Ruan, Y. Wu, J. Kong, J. Gu, Enhanced thermal conductivities and decreased thermal resistances of functionalized boron nitride/polyimide composites, Compos. Part B Eng. 164 (2019) 732–739. https://doi.org/10.1016/j.compositesb.2019.01.099.

[33] C.A. Gueymard, The sun's total and spectral irradiance for solar energy applications and solar radiation models, Sol. Energy. 76 (2004) 423–453. https://doi.org/10.1016/j.solener.2003.08.039.

[34] S. Wang, J. Zhang, Effect of titanium dioxide (TiO2) on largely improving solar reflectance and cooling property of high density polyethylene (HDPE) by influencing its crystallization behavior, J. Alloys Compd. 617 (2014) 163–169. https://doi.org/10.1016/j.jallcom.2014.07.191.

[35] J. Wang, Y. Li, L. Deng, N. Wei, Y. Weng, S. Dong, D. Qi, J. Qiu, X. Chen, T. Wu, High-Performance Photothermal Conversion of Narrow-Bandgap Ti2O3Nanoparticles, Adv. Mater. 29 (2017) 1–6. https://doi.org/10.1002/adma.201603730.

[36] X. Lu, H. Huang, X. Zhang, P. Lin, J. Huang, X. Sheng, Novel light-driven and electro-driven polyethylene glycol / two-dimensional MXene form-stable phase change material with enhanced thermal conductivity and electrical conductivity for thermal energy storage, Compos. Part B. 177 (2019) 107372. https://doi.org/10.1016/j.compositesb.2019.107372.

[37] T. Qian, J. Li, W. Feng, Single-walled carbon nanotube for shape stabilization and enhanced phase change heat transfer of polyethylene glycol phase change material, Energy Convers. Manag. 143 (2017) 96–108. https://doi.org/10.1016/j.enconman.2017.03.065.

[38] C. Wang, L. Feng, W. Li, J. Zheng, W. Tian, X. Li, Shape-stabilized phase change materials based on polyethylene glycol/porous carbon composite: The influence of the pore structure of the carbon materials, Sol. Energy Mater. Sol. Cells. 105 (2012) 21–26. https://doi.org/10.1016/j.solmat.2012.05.031.

[39] C. Li, B. Xie, D. Chen, J. Chen, W. Li, Z. Chen, S.W. Gibb, Y. Long, Ultrathin graphite sheets stabilized stearic acid as a composite phase change material for thermal energy storage, Energy. 166 (2019) 246–255. https://doi.org/10.1016/j.energy.2018.10.082.

[40] C. Li, B. Xie, J. Chen, Graphene-decorated silica stabilized stearic acid as a thermal energy storage material, RSC Adv. 7 (2017) 30142–30151. https://doi.org/10.1039/c7ra05204a.

[41] F. Bahiraei, A. Fartaj, G.A. Nazri, Experimental and numerical investigation on the performance of carbon-based nanoenhanced phase change materials for thermal management applications, Energy Convers. Manag. 153 (2017) 115–128. https://doi.org/10.1016/j.enconman.2017.09.065.

[42] M. George, A.K. Pandey, N. Abd, V. V Tyagi, S. Shahabuddin, R. Saidur, A novel polyaniline (PANI)/ para ffi n wax nano composite phase change material : Superior transition heat storage capacity , thermal conductivity and thermal reliability, Sol. Energy. 204 (2020) 448–458. https://doi.org/10.1016/j.solener.2020.04.087.

[43] A. Arshad, M. Jabbal, Y. Yan, Thermophysical characteristics and application of metallic-oxide based mono and hybrid nanocomposite phase change materials for thermal management systems, Appl. Therm. Eng. 181 (2020) 115999. https://doi.org/10.1016/j.applthermaleng.2020.115999.

[44] H. Babaei, P. Keblinski, J.M. Khodadadi, Thermal conductivity enhancement of paraffins by increasing the alignment of molecules through adding CNT/graphene, Int. J. Heat Mass Transf. 58 (2013) 209–216. https://doi.org/10.1016/j.ijheatmasstransfer.2012.11.013.

[45] A. Karaipekli, A. Biçer, A. Sarı, V. Veer, Thermal characteristics of expanded perlite / paraffin composite phase change material with enhanced thermal conductivity using carbon nanotubes, Energy Convers. Manag. 134 (2017) 373–381. https://doi.org/10.1016/j.enconman.2016.12.053.